

Design of a High-Bandwidth Rogowski Current Sensor for Gate-Drive Shortcircuit Protection of 1.7 kV SiC MOSFET Power Modules

Jun Wang, Zhiyu Shen, Rolando Burgos, Dushan Boroyevich
Center for Power Electronics Systems
Virginia Polytechnic Institute and State University
Blacksburg, VA 24061, USA
junwang@vt.edu

Abstract—This presents a PCB-based Rogowski current sensor design for the purpose of shortcircuit protection for 1.7 kV SiC MOSFET modules. Firstly, the paper shows that using the DeSat protection method for SiC MOSFET protection is not as effective as that in conventional IGBT applications. Therefore, a direct measurement of device switching current is proposed to achieve shortcircuit protection. The Rogowski-coil-based current sensor is selected among several high-bandwidth candidates for its better overall performance. Then the PCB-based Rogowski coil and its signal processing circuit design are shown in the paper. Finally, experimental results validate that the designed sensor has good performance in both accuracy and bandwidth when compared to a commercial Rogowski probe.

Keywords—SiC MOSFET; shortcircuit protection; Rogowski coil; high bandwidth current sensor

I. INTRODUCTION

SiC MOSFET as a wide-bandgap device has superior performance for its high breakdown electric field, low on-state resistance, fast switching speed and high working temperature [1]. High switching speed enables high switching frequency, which improves the power density of high power converters. The cost of SiC MOSFET is also gradually decreasing due to the growing of usage in industry applications. In addition, the development of packaging technology for the device let the device be able to take more current as a packaged module. Therefore, all of the above facts bring a promising trend to replace the conventional IGBTs with SiC MOSFETs in high power applications.

High dv/dt , brought by the fast switching speed, usually leads to a high likelihood to induce the cross-talk issue. It can create a shortcircuit event to damage the device. Since the SiC MOSFET module is more expensive compared to IGBT with the same ratings, the damage of the SiC MOSFET is not usually affordable. Thus, the device shortcircuit protection is of great importance in practical applications. The most conventional method to protect IGBTs from overcurrent is the DeSat protection by detecting the on-state device voltage, which is related to the device current according to its output characteristics. In recent protection designs for SiC MOSFET, the DeSat method is simply borrowed from the IGBT applications. However, DeSat protection for SiC MOSFET is not as effective as it is for IGBT because of two main reasons.

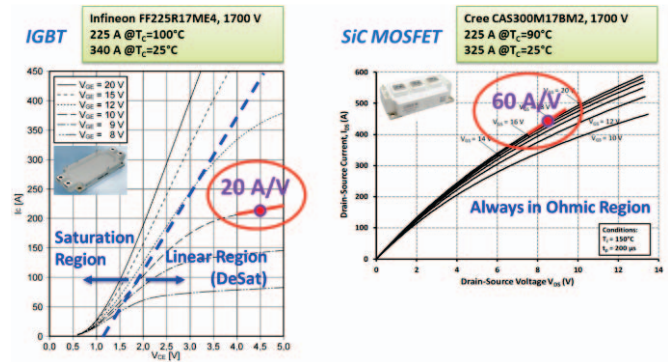


Fig. 1. Device output characteristics comparison, IGBT vs. SiC MOSFET

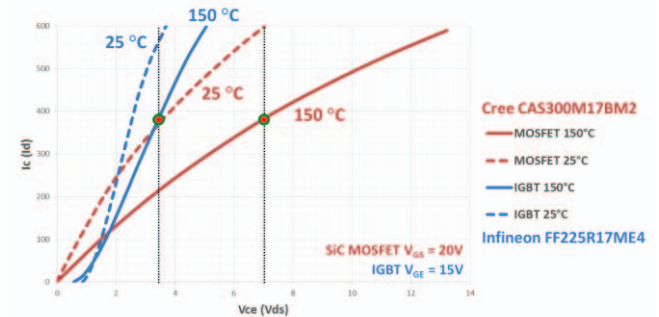


Fig. 2. Device output characteristics comparison against junction temperature

1) As shown in Fig.1, when overcurrent occurs in IGBTs, the device drifts away from the saturation region and goes into linear region where the current rising slope is getting smaller. The in-time shut down can be achieved easily even with detection delays and sensing errors because the current won't increase very fast at linear region. In contrast, however, The SiC MOSFET is still in its Ohmic region where the current rising slope is much faster than IGBTs. Then delays or on-state voltage sensing errors can lead to higher possibility of device damage before it can be shut-down in time and safely.

2) As shown in Fig.2, the output characteristics curve of the two type of device shows that the on-state voltage of the SiC MOSFET is more temperature dependent than that of the IGBT. If a DeSat protection is designed for the nominal junction temperature, then it can hardly be effective when the

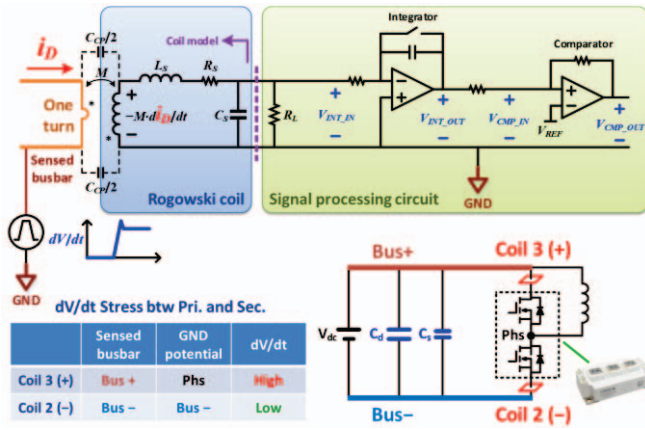


Fig. 3. Conductive noise due to high dv/dt

device temperature is still low at the startup of the converter. Instead, if the protection is designed for low junction temperature, then it can be possibly falsely triggered at nominal junction temperatures and stop the converter from normal operations. As a result, the distinctive difference between two output characteristics curves in different temperature of the SiC MOSFET make it very difficult to design DeSat threshold voltage.

As the DeSat protection may not function well for SiC MOSFET, a current sensor is a good additional option to detect the fault current. Reference [2] reviews and compares different current sensing method, including shunt, Hall, current transducer, Rogowski coil, GMR and GMI, concluding that the Rogowski coil has outstanding performances in terms of bandwidth, accuracy, linearity, implementation, profile and cost. Another alternative method to detect the overcurrent is to take advantage of the stray inductance between the Kelvin pin and the power terminal of the emitter was validated in IGBT applications [3]. The stray inductance voltage carries the di/dt information of the device that can be used to derive the current information. However, this method is highly package-dependent without guarantee to provide clear di/dt information against noise.

Rogowski current sensor is applied in IGBT current sensing for overcurrent protection or current sharing in device-parallel applications [4]. It is also designed for discrete SiC MOSFET device [5]. In this paper, a Rogowski current sensor is designed for Cree 1.7 kV SiC MOSFET modules with part number of CAS300M17BM2. Impact from the high dv/dt noise and adjacent current noise is considered during the design. An active reset circuit is also designed to guarantee that the sensor can measure DC current. The performance of the designed Rogowski current sensor is validated to be good in comparison to a commercial Rogowski probe CWT3B.

II. ROGOWSKI SENSOR DESIGN CHALLENGES

A. Conductive noise due to high dv/dt

The equivalent circuit model of the Rowoski coil and signal processing circuit is show in Fig. 3. The PCB-based Rogowski coil is sitting on top of the DC terminals of the SiC MOSFET

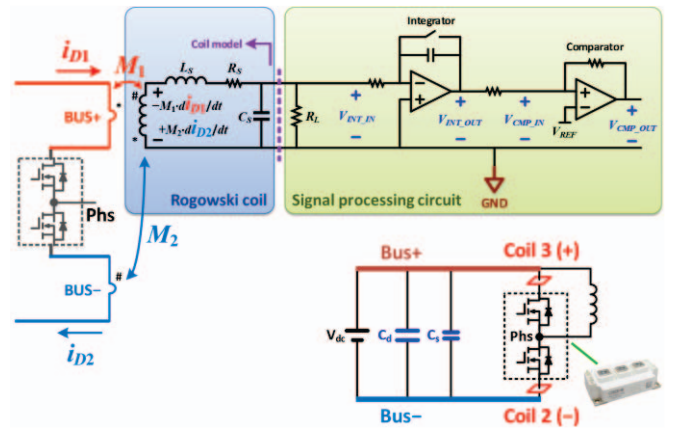


Fig. 4. Radiated noise from adjacent conductors

module, while the sensor circuit will be grounded to the source terminal of the device whose current is measured by the sensor. Therefore, the voltage difference between the device busbar and sensor ground will be the device voltage, which has a large dv/dt when switching the SiC device. The analysis in Fig. 3 shows that this dv/dt noise will be critical for the high-side device measurement. A common-mode (CM) noise current will flow from the device busbar to the sensor circuit through the coupling capacitance C_{CP} , introducing sensing error in the device measurement. Therefore, very careful PCB layout design should be carried out to bypass the CM noise current from the sensing circuit.

B. Radiated noise from adjacent conductors

The power connections to the device module terminals is usually very close to each other, so the negative conductor will be located adjacent to the positive Rogowski coil, and vice versa. Then the induced voltage on the coil output will carry both the positive and negative busbar current information. A compensation winding is usually designed in the Rogowski coil to minimize the noise from adjacent conductors [6]. Also, the turn number of the winding has influence on the coupling effect from the adjacent conductor, which should be carefully designed.

III. COIL AND SIGNAL PROCESSING CIRCUIT DESIGN

A. Rogowski coil design

Because of the limited space between the two power terminals of the Cree module, the winding width is designed to be 1 mm. In order to minimize the noise from adjacent conductors, the coil surrounds the terminal busbar, and has a one-turn winding to compensate the one-turn effect of the coil. The PCB design in shown in Fig. 5 and the physical assembly is shown in Fig.6. Three different winding designs are simulated in Ansoft Q3D. It can be observed from the results that higher turn number of the winding will lead to less coupling effect from the adjacent busbar. The maximum turn number that can be physically achieved is 176 turns based on normal PCB manufacturing techniques. Winding mutual inductance M_1 , self-inductance L_S and AC resistance R_S is

	Design A	Design B	Design C
Turn Number	44	88	176 (max.)
M1 to BUS+	0.725 nH	1.327 nH	1.839 nH
M2 to BUS-	0.089 nH (12.3%)	0.116 nH (8.7%)	0.138 nH (7.5%) ✓
L_s	116 nH	198 nH	363 nH
R_s @20MHz	0.88 Ω	1.56 Ω	2.23 Ω
C_p	1.16 pF (Bus+)	1.19 pF (Bus-)	1.31 pF (Bus+)
	1.19 pF (Bus-)	1.34 pF (Bus+)	1.34 pF (Bus-)
	1.34 pF (Bus+)	1.20 pF (Bus-)	

Fig. 5. Comparison of three Rogowski-coil designs

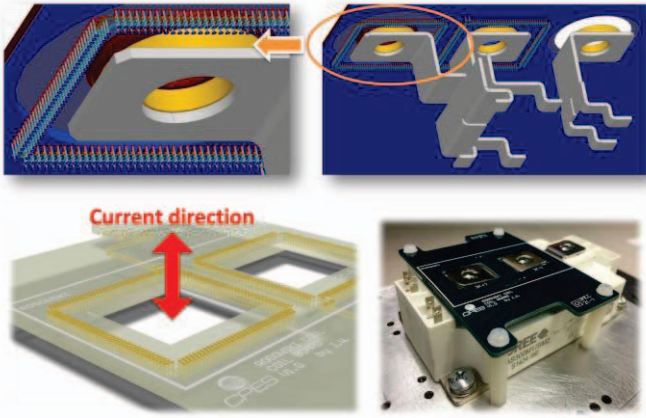


Fig. 6. Rogowski coil 3D model and assembly

shown in Fig.6 which is used in the later parameter design of signal processing circuit.

B. Signal processing circuit design

Signal processing circuit is designed to integrate the di/dt information obtained from the Rogowski coil output. Active integration circuit using operational amplifier is selected instead of RC passive signal circuit to achieve wider sensor bandwidth [7]. The output of the integrator circuit is sent to a low-propagation-delay comparator. The output of the comparator is given to high-voltage (secondary) side of the isolated gate driver IC to switch off the SiC MOSFET as soon as the comparator input voltage V_{CMP_IN} exceed the threshold voltage V_{REF} . The propagation delay from the device current I_D to the comparator output V_{CMP_OUT} is designed to be less than 20 ns.

Input resistor R_{I1} and integration capacitor C_f determines the transducer gain G_{SENSOR} from device current I_D to comparator input V_{CMP_IN} according to (1). Note that the di/dt polarities of the positive and negative busbar are opposite, while the values are identical with negligible equivalent paralleled capacitance (EPC) of the phase inductor. Therefore, the equivalent mutual inductance is the different between the mutual inductance from the measured conductor and the adjacent conductor.

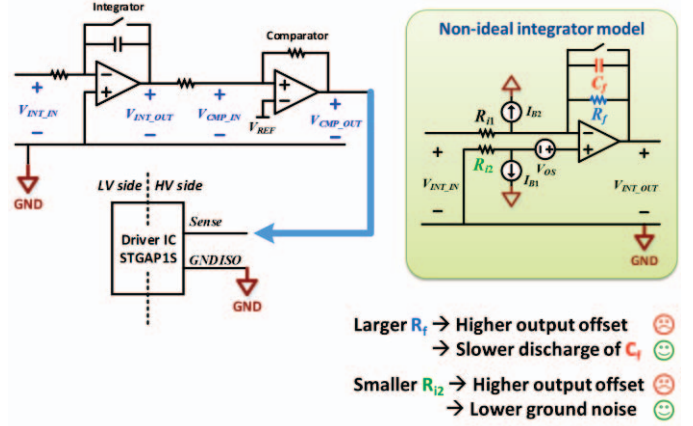


Fig. 7. Signal processing circuit diagram and non-ideal integrator model

$$G_{SENSOR} = (M_1 - M_2) / (R_{I1} \cdot C_f) \quad (1)$$

Larger C_f is preferred to prevent integration error caused by C_f discharging. It is finally fine-tuned that $R_{I1} = 403 \Omega$ and $C_f = 200 \text{ pF}$ to achieve $G_{SENSOR} = 0.02 \Omega$. Then the mutual inductance is calculated to be $M_1 - M_2 = 1.61 \text{ nH}$, which is very close to the simulation result 1.70 nH. The reasonable error is likely caused by the difference between the simulation model and the real assembly.

The general non-idea characteristics of an operational amplifier can be modeled as shown in Fig. 7. The bias current I_{B1} and I_{B2} and offset voltage V_{OS} cause an output voltage offset at V_{OUT} even when the input voltage to V_{IN} is zero. In conventional designs, the feedback resistor R_f is designed to minimize the effect from offset voltage V_{OS} , and two identical input resistors R_{I1} and R_{I2} is selected to cancel out the effect of from bias current I_{B1} and I_{B2} . The larger R_f leads to higher output offset, but to slower discharge of the C_f such that the sensor gain will not decrease if the device conducting time is long. The smaller R_{I2} leads to higher output offset, but to lower ground noise at the non-inverting input terminal of operational amplifier. Eventually, the R_f is designed to be infinite (open circuit) and R_{I2} is zero, in order to maximize the sensing performance. The output offset issue can be resolved by the active reset switch. The reset switch is designed to turn on for a very short time when the SiC MOSFET is switched off. A bidirectional analog switch is selected with on-state resistance 6.3Ω and switch time of 25 ns, which can discharge of the capacitor C_f within 30 ns for SiC MOSFET in high switching-frequency applications.

IV. EXPERIMENTAL VALIDATION

The test of the Rogowski coil and the signal processing circuit has been carried out in a Double-Pulse Test (DPT) setups shown in Fig. 8. Fig. 9 shows that 5 pulses are fired to validate the transient performances and the reset function. Since the reset signal is designed to be given after the turn-off of the SiC MOSFET, the first current pulse is captured on basis of the DC offset voltage, and the following 4 pulses are captured starting from zero volt. During the test, the external gate resistor is selected to be almost zero such that the

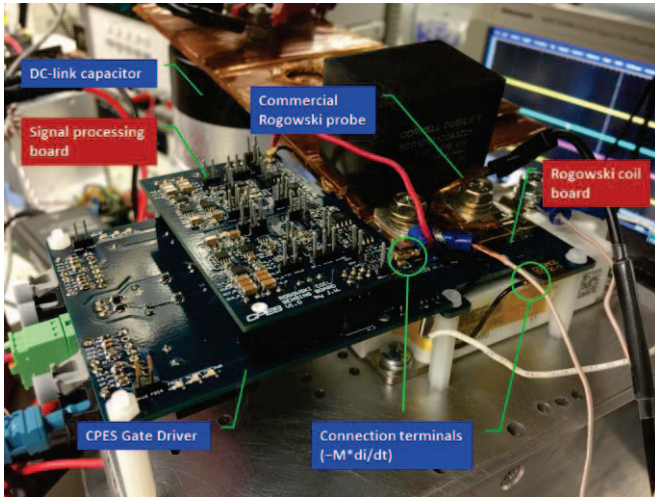


Fig. 8. Test setup and circuit boards

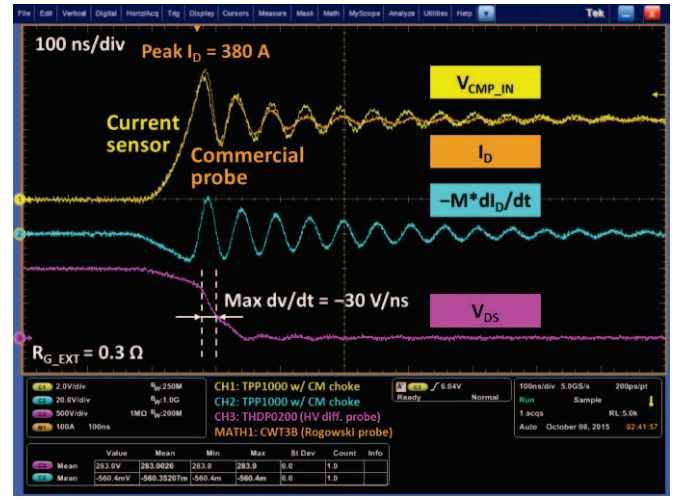


Fig. 10. Switch-on performance of the Rogowski current sensor

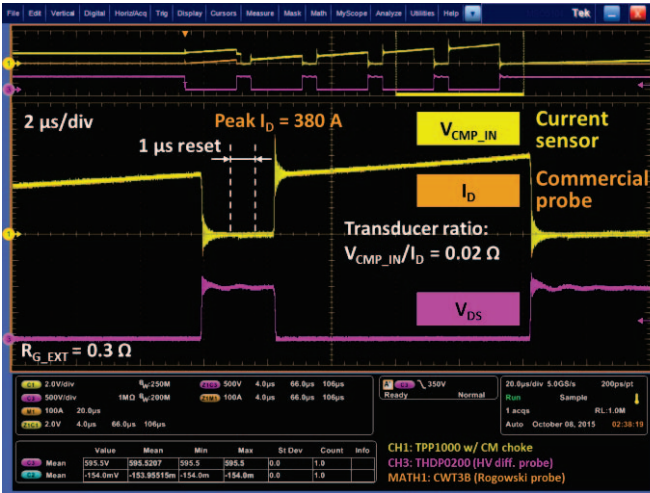


Fig. 9. Switching transient performances of the Rogowski current sensor

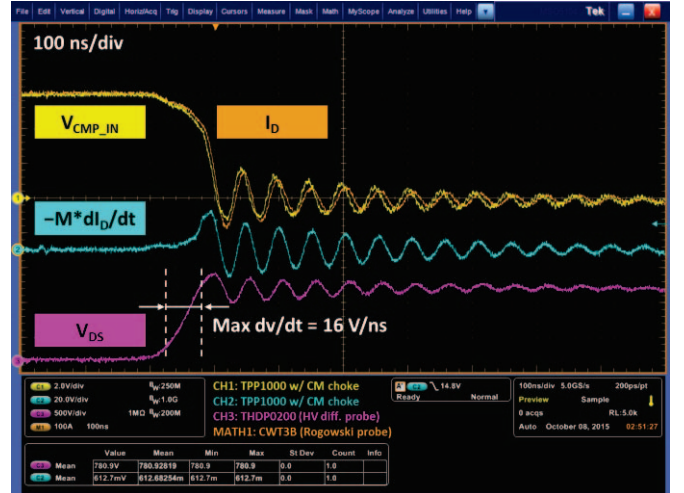


Fig. 11. Switch-off performance of the Rogowski current sensor

maximum turn-on dv/dt reaches 30 V/ns, as shown in Fig. 10. The turn-on performance of the sensor almost has almost the same delay of the commercial Rogowski probe, but has higher-magnitude high-frequency ringing at about 16 MHz. Note that the band width of the probe CWT3B is 20 MHz, so its gain at 16 MHz probably begin to drop. However, the designed sensor uses 120 MHz operational amplifier that provide higher bandwidth than the commercial probe. In Fig. 11, the turn-off performance shows that the designed sensor has even less delay time than the commercial probe.

V. CONCLUSIONS

A PCB-based Rogowski current sensor for 1.7 kV SiC MOSFET module has been designed, built and tested. The test results show that the sensor have even better performance than the commercial Rogowski probe at high dv/dt environment.

REFERENCES

- [1] J. Millan, P. Godignon, X. Perpina, A. Perez-Tomas, J. Rebollo, "A survey of wide bandgap power semiconductor devices," *IEEE Trans. Power Electron.*, vol. 29, no. 5, pp. 2155-2163, May, 2014.
- [2] C. Xiao, L. Zhao, T. Asada, W. G. Odendaal, and J. D. van Wyk, "An overview of integratable current sensor technologies," in 2003, vol. 2, pp. 1251-1258.
- [3] Z. Wang, X. Shi, L.M. Tolbert, F. Wang, and B.J. Blalock, "A di/dt feedback-based active gate driver for smart switching and fast overcurrent protection of IGBT modules," *IEEE Trans. Power Electron.*, vol.29, no.7, pp.3720-3732, July, 2014.
- [4] D. Bortis, J. Biela, and J. W. Kolar, "Active gate control for current balancing of parallel-connected IGBT modules in solid-state modulators," *IEEE Trans. Plasma Sci.*, vol. 36, pp. 2632-2637, 2008.
- [5] Y. Xue, J. Lu, Z. Wang, L.M. Tolbert, B.J. Blalock, and F. Wang, "A compact planar Rogowski coil current sensor for active current balancing of parallel-connected Silicon Carbide MOSFETs," in *Proc. IEEE Electr. Power. Energy Conf.*, pp.4685-4690, Sept., 2014.
- [6] T. Guillod, D. Gerber, J. Biela, and A. Muesing, "Design of a PCB Rogowski coil based on the PEEC method," in *Proc. IEEE Integrated Power Electron. Sys.*, 2012, pp. 1-6.
- [7] W. F. Ray and C. R. Hewson, "High performance Rogowski current transducers," in *Proc. IEEE Ind. Applic. Conf.*, 2000, vol. 5, pp. 3083-3090.